International Journal of Thermophysics, Vol. 20, No. 2, 1999

The Equation of State of Song and Mason Applied to Fluorine

H. Eslami[1,2] and A. Boushehri[1]

Received June 23, 1998

An analytical equation of state is applied to calculate the compressed and saturation thermodynamic properties of fluorine. The equation of state is that of Song and Mason. It is based on a statistical-mechanical perturbation theory of hard convex bodies and is a fifth-order polynomial in the density. There exist three temperature-dependent parameters: the second virial coefficient, an effective molecular volume, and a scaling factor for the average contact pair distribution function of hard convex bodies. The temperature-dependent parameters can be calculated if the intermolecular pair potential is known. However, the equation is usable with much less input than the full intermolecular potential, since the scaling factor and effective volume are nearly universal functions when expressed in suitable reduced units. The equation of state has been applied to calculate thermodynamic parameters including the critical constants, the vapor pressure curve, the compressibility factor, the fugacity coefficient, the enthalpy, the entropy, the heat capacity at constant pressure, the ratio of heat capacities, the Joule–Thomson coefficient, the Joule–Thomson inversion curve, and the speed of sound for fluorine. The agreement with experiment is good.

KEY WORDS: equation of state; fluorine; thermodynamic properties.

1. INTRODUCTION

Fluorine, the most chemically reactive element of the periodic table, was isolated more than a century ago by Moissan [1], who received a Noble Prize for this achievement. It has widespread applications in modern

[1] Department of Chemistry, Shiraz University, Shiraz 71454, Iran.
[2] To whom correspondence should be addressed.

0195-928X/99/0300-0611$16.00/0

industry and technology. One of the main current uses for elemental fluorine is in the nuclear power industry for the production of uranium hexafluoride which is needed for the separation, by gaseous diffusion, of ^{235}U. An expanding use is in the manufacture of sulfur hexafluoride, which is widely used in power generation and distribution industries as an insulator in gas-filled circuit breakers and as the main insulation for power transmission in high-voltage coaxial cables. A new use is in the development of a high-powered laser which burns hydrogen and fluorine gases to form hot hydrogen fluoride molecules which emit infrared light at a wavelength of 2.7 μm.

A central problem in the theory of fluids is the relation of their thermodynamic parameters in terms of intermolecular forces. One of the fundamental approaches to this problem is through the formulation of an accurate equation of state, since the thermodynamic functions can be easily derived once the equation of state is known. The most successful theories at present are perturbation theories based on reference systems consisting of hard bodies [2] analogous to the perturbation theories of simple fluids based on hard spheres. Two different methods are primarily used in these theories, depending on the type of pair potentials used to characterize molecular interactions, the multicenter potential [3] and the Kihara core potential [4]. The respective perturbation theories employ fused hard spheres or hard convex bodies as reference systems. Unfortunately, both types of theories require considerable numerical computations and no simple analytical equation of state for molecular fluids is available.

Recent work by Song and Mason on a statistical–mechanical theory for the equation of state of fluids has yielded simple but remarkably accurate results for both spherical [5] and molecular [6] fluids. Three temperature-dependent parameters arise in their formulation: the second virial coefficient, an effective hard-sphere diameter, and a scaling factor for the pair distribution function at contact. All three parameters can be calculated from the intermolecular potential. If the intermolecular potential is not known, the last two parameters can be determined from the experimental second virial coefficient because they are insensitive to the shape of the potential. Thus, the second virial coefficient serves to predict the entire equation of state in terms of two scaling parameters and, hence, a number of other thermodynamic properties including the enthalpy, the internal energy, and the vapor pressure curve among others. The purpose of this paper is to apply this equation of state to calculate compressed and saturation thermodynamic properties of fluorine. It should be noted that the accuracy is not necessarily enhanced by greater complexity of the equation of state.

2. THEORY

Song and Mason [6] obtained an analytical equation of state for convex-molecule fluids based on statistical–mechanical perturbation theory. The equation of state is of the form,

$$\frac{p}{\rho kT} = 1 + B_2(T)\,\rho + \alpha(T)\,\rho[G(\eta) - 1] \tag{1}$$

where p is the pressure, ρ is the molar (number) density, $B_2(T)$ is the second virial coefficient, $\alpha(T)$ is the contribution of the repulsive forces to the second virial coefficient, $G(\eta)$ is the average pair distribution function at contact for equivalent hard convex bodies, and kT has its usual meaning. They adopted the following form for $G(\eta)$, which was found to be accurate for hard convex bodies [6, 7],

$$G(\eta) = \frac{1 - \gamma_1\eta + \gamma_2\eta^2}{(1-\eta)^3} \tag{2}$$

where γ_1 and γ_2 are chosen to reproduce the correct third and fourth virial coefficients of the bodies and η is the packing fraction. In practice γ_1 and γ_2 can be approximated in terms of a single nonsphericity parameter γ, equal to unity for hard spheres. The parameters γ_1 and γ_2 have been defined in terms of γ as [6]

$$\gamma_1 = 3 - \frac{1 + 6\gamma + 3\gamma^2}{1 + 3\gamma} \tag{3}$$

$$\gamma_2 = 3 - \frac{2 + 2.64\gamma + 7\gamma^2}{1 + 3\gamma} \tag{4}$$

The packing fraction, η, is given by

$$\eta = \frac{b\rho}{1 + 3\gamma} \tag{5}$$

where b is the van der Waals covolume and can be defined in terms of α as

$$b = \alpha + T\frac{d\alpha}{dT} \tag{6}$$

Once the intermolecular potential is known, the parameters $B_2(T)$, $\alpha(T)$, and $b(T)$ can be found by integration:

$$B_2(T) = 2\pi \int_0^{\infty} (1 - e^{-u/kT})\, r^2\, dr \tag{7}$$

$$\alpha(T) = 2\pi \int_0^{r_m} (1 - e^{-u_0/kT})\, r^2\, dr \tag{8}$$

where $u_0(r)$ is the repulsive part of $u(r)$.

In practice, the potential $u(r)$ is seldom accurately known, although $B_2(T)$ itself can be found experimentally. In such cases Eq. (1) can be treated as an equation of state with two unknown temperature-dependent parameters, α and b. However, it turns out that α and b are rather insensitive to the shape of $u(r)$, so that they appear as almost universal functions of temperature in terms of suitable reduced units.

Suitable reduced units can be chosen by imagining that $B_2(T)$ is known and that the parameters ε and r_m for some model potential $u(r)$ are found by fitting B_2, preferably in the region of the Boyle temperature. The values of ε and r_m will depend on the particular model chosen, but they will always be such as to reproduce the values of the Boyle temperature T_B, the Boyle volume v_B, and the Boyle pressure p_B, defined as

$$B_2(T_B) = 0, \qquad v_B = T_B \left(\frac{dB_2}{dT}\right)_{T_B}, \qquad p_B = kT_B/v_B \tag{9}$$

The reduced quantities α/v_B and b/v_B turn out to be almost universal functions of the reduced temperature, T/T_B, and depend only weakly on the detailed shape of $u(r)$. They can therefore be calculated on the basis of some simple mean spherical potential such as the Lennard–Jones (12–6) potential, and numerical tables giving α/v_B and b/v_B as functions of T/T_B for the (12–6) potential are available [5].

If data for $B_2(T)$ do not extend to high enough temperatures to determine T_B and v_B directly, an extrapolation procedure with a mean-spherical potential can be used. Such a potential can be defined via $B_2(T)$ as Eq. (7). This integral is evaluated for some choice of $u(r)$, and then the average potential parameters ε and r_m for $u(r)$ are found by fitting the experimental $B_2(T)$, preferably as close as possible to the Boyle temperature. Then T_B and v_B follow directly from ε and r_m for the particular potential chosen.

The remaining parameter γ is best found by fitting available $p - v - T$ data, preferably at high densities. Since γ is thus determined empirically, it tends to compensate for any inaccuracies in the values adopted for T_B and

v_B or, equivalently, for any inadequacies in the form chosen for $u(r)$ and resultant inaccuracies in the values of ε and r_m.

3. COMPARISON WITH EXPERIMENT

3.1. Thermodynamic Properties in the Compressed State

Because of the above-mentioned applications of fluorine we decided to calculate its thermodynamic properties. We used accurate values of $B_2(T)$ [8] for calculating the Lennard–Jones (12–6) parameters. Since the experimental values of $B_2(T)$ for fluorine [8] do not extend to the Boyle temperature, we used the above-mentioned procedure to determine average potential parameters via Eqs. (7) and (9) and then the Boyle parameters were calculated. We obtained $\varepsilon/k = 108.747$ K, $r_m = 3.742$ Å, $T_B = 371.7$ K, and $v_B = 37.91$ ml · mol^{-1}. In determining the Boyle parameters, the tabulated values of α/v_B and b/v_B as a function of T/T_B for the (12–6) potential [5] were used. The parameter γ is then found by fitting the high-density experimental p–v–T data [9] for fluorine. The p–v isotherms are shown in Fig. 1 at three temperatures, one below and two above the critical temperature, for the best calculated value of γ, that is, $\gamma = 1.118$.

3.1.1. Compressibility Factor

The compressibility factor, defined as $Z = p/\rho kT$, shows the extent of deviation from ideality. Once the equation of state is known, the

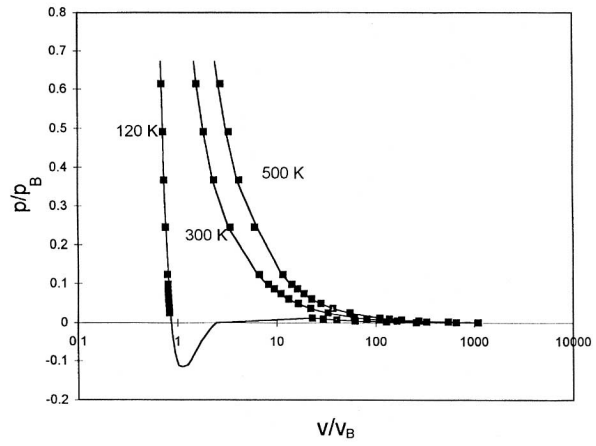

Fig. 1. Reduced p–v isotherms. The curves represent the equation of state, and the points indicate the experimental data [9].

compressibility factor can be calculated at any temperature and pressure. Compressibility isotherms have been calculated from the equation of state over the pressure range of 1 to 500 bar and are compared with the calculated (smoothed) values of de Reuck [10] in Fig. 2. The agreement is within $\pm 2\%$.

3.1.2. Fugacity Coefficient

The fugacity is related to the equation of state by the formula

$$\ln \frac{f}{p} = kT \int_0^p (Z-1) \frac{dp}{p} \tag{10}$$

where f is the fugacity and Z is the compressibility factor. The ratio f/p is called the fugacity coefficient. The fugacity coefficient can be calculated from Eq. (10) in conjunction with the equation of state. Since the analytical calculation of the above integral is not straightforward, we proceeded numerically. The calculated isotherms of the fugacity coefficient over the pressure range of 1 to 500 bar and their good agreement (within $\pm 1.7\%$) with the calculated values in Ref. 10 are shown in Fig. 3.

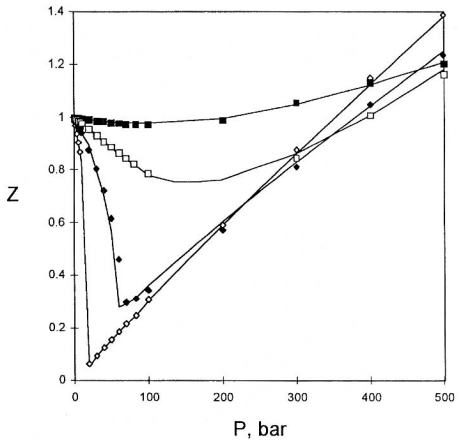

Fig. 2. The plot of compressibility factor, Z, as a function of pressure at 110 K (◇), 150 K (◆), 200 K (□), and 300 K (■). The curves represent the equation of state, and the points are taken from Ref. 10. The points above 200 bar are taken from Ref. 9.

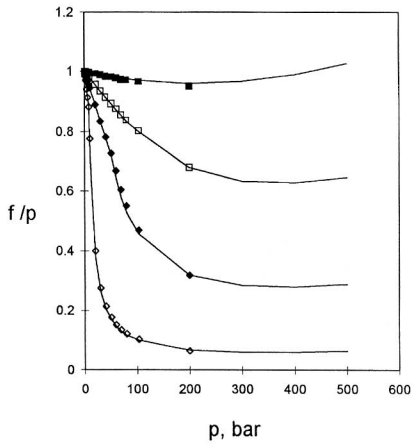

Fig. 3. Same as Fig. 1 for the fugacity coefficient, f/p.

3.1.3. Enthalpy

The excess internal energy can be found from

$$U^{ex} = \int_0^\rho \frac{1}{\rho^2}\left[p - T\left(\frac{\partial p}{\partial T}\right)_v \right] d\rho \tag{11}$$

This yields

$$\frac{U^{ex}}{NkT} = -\rho T \frac{dB_2}{dT} + \frac{(1+3\gamma)}{b}\left\{(b-\alpha)\left[-\frac{[2-(1+\gamma_1)\eta - \gamma_2(2-3\eta)]\eta}{2(1-\eta)^2} + \eta + \gamma_2 \ln(1-\eta)\right] - \frac{\alpha}{b} T \frac{db}{dT}\left[\gamma_2 \ln(1-\eta) + \frac{(3-\gamma_1)\eta^2 - (1-\gamma_1)\eta^3 + \gamma_2(2-5\eta+5\eta^2)\eta}{2(1-\eta)^3}\right]\right\} \tag{12}$$

The excess internal energy is the internal energy relative to the ideal gas at the same temperature and pressure. The internal energy can be found by adding the excess internal energy and the internal energy of the ideal gas, which can be calculated via the following equation [11].

$$\frac{U}{NkT} = \frac{5}{2} + \frac{h\nu/kT}{e^{h\nu/kT} - 1} - \frac{D_e}{kT} \tag{13}$$

where h is Planck's constant, ν is the vibrational frequency, and D_e is the dissociation energy.

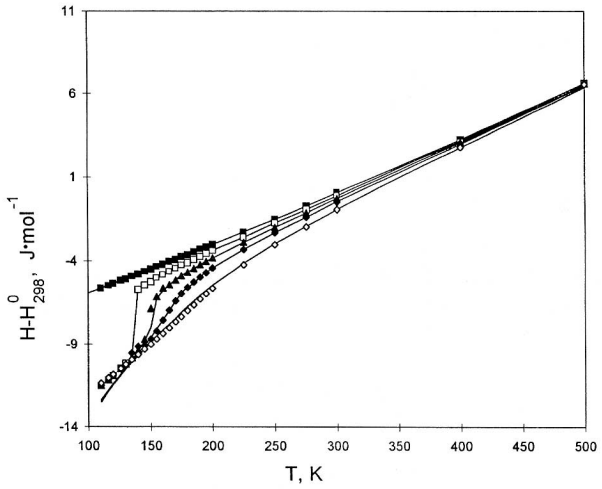

Fig. 4. The enthalpy, $H-H^0_{298}$, as a function of temperature at 1 bar (■), 30 bar (□), 60 bar (▲), 100 bar (◆), and 200 bar (◇). The curves represent the equation of state, and the points are taken from Ref. 10. The points above 100 K are taken from Ref. 9.

The enthalpy can be found by the equation, $H = U + pv$. Since enthalpy does not have an absolute value, it is necessary to choose a zero reference state (p_0, T_0) from which the difference in enthalpy can be calculated. The zero reference state is taken to be (1 bar, 298 K), and the enthalpy of fluorine at this state is 8.825 kJ·mol^{-1} [10]. We have calculated the molar enthalpies of the liquid and vapor phases relative to the molar enthalpy of the ideal gas at 298 K. The vibrational frequency and dissociation energy of fluorine are 918 cm^{-1} and 160 kJ·mol^{-1}, respectively [12]. Shown in Fig. 4 are the isobars of enthalpy and their comparison with the calculated values in Ref. 10. The average absolute deviation for the higher-pressure isobar over the temperature range of 100 to 500 K is 3%.

3.1.4. Entropy

The excess entropy is the entropy relative to the entropy of the ideal gas at the same temperature and pressure and is defined as

$$\frac{S^{ex}}{Nk} = \int_0^\rho \frac{1}{\rho^2}\left[\left(\frac{\partial p}{\partial T}\right)_\rho - \rho\right] d\rho \tag{14}$$

where S^{ex} is the excess entropy. For the present equation of state, this yields

$$\frac{S^{ex}}{Nk}=\left(b-B_2-T\frac{dB_2}{dT}\right)\rho+(1+3\gamma)$$
$$\times\left\{\left[\gamma_2\ln(1-\eta)-\frac{(3\gamma_2-\gamma_1-1)\eta^2+2(1-\gamma_2)\eta}{2(1-\eta)^2}\right]-\frac{\alpha}{b^2}T\frac{db}{dT}\right.$$
$$\left.\times\left[\gamma_2\ln(1-\eta)+\frac{(5\gamma_2-\gamma_1-1)\eta^3+(3-\gamma_1-5\gamma_2)\eta^2+2\gamma_2\eta}{2(1-\eta)^3}\right]\right\} \quad (15)$$

The entropy S can be calculated by adding the excess entropy to the entropy of the ideal gas [11] at the same temperature and pressure via the following equation.

$$\frac{S}{Nk}=\frac{S^{ex}}{Nk}+\ln\left(\frac{2\pi mkT}{h^2}\right)^{3/2}\frac{e^{5/2}}{\rho N}+\ln\frac{8\pi^2IkTe}{\sigma h^2}$$
$$+\frac{h\nu/kT}{e^{h\nu/kT}-1}-\ln(1-e^{-h\nu/kT})+\ln w_{el} \quad (16)$$

where m is the molecular weight, I is the moment of inertia, σ is the symmetry number, and w_{el} is the ground electronic state degeneracy.

The isobars of S–S^0_{298} have been calculated with Eqs. (1), (15), and (16), and they are compared with the calculations of de Reuck [10] in Fig. 5.

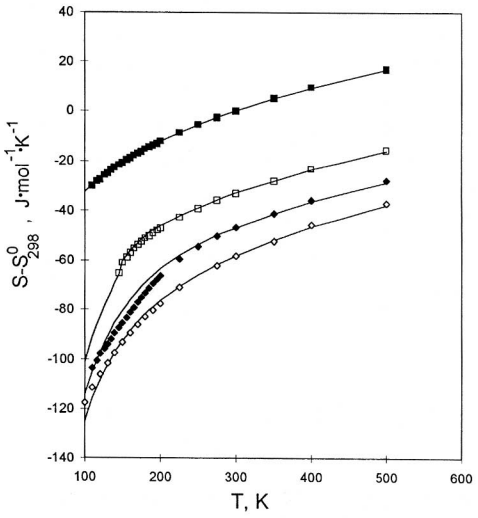

Fig. 5. Same as Fig. 4 for the entropy at 1 bar (■), 50 bar (□), 200 bar (◆), and 500 bar (◇). The points at temperatures above 300 K and pressures above 200 bar are taken from Ref. 9.

The entropy of fluorine at 1 bar and 298 K is 202.791 $J \cdot mol^{-1} \cdot K^{-1}$ [10], and the equilibrium internuclear distance for calculating the moment of inertia is 1.41 Å [12]. The ground electronic state of fluorine is nondegenerate, and the symmetry number is 2. The maximum deviations extend to $\pm 15.2\%$ over the temperature range of 100 to 500 K.

3.1.5 Heat Capacities

The heat capacity at constant volume is defined as

$$C_v = T\left(\frac{\partial S}{\partial T}\right)_v \tag{17}$$

For the present equation of state C_v is

$$\begin{aligned} C_v = &\left(T\frac{db}{dT} - 2T\frac{dB_2}{dT} - T^2\frac{d^2B_2}{dT^2}\right)\rho - \frac{(1+3\gamma)}{b}\left\{T\frac{db}{dT}\left[\gamma_2 \ln(1-\eta)\right.\right. \\ &\left. + \frac{(7\gamma_2 - \gamma_1 - 1)\eta^3 + (3 - 3\gamma_1 - 5\gamma_2)\eta^2 + 2(\gamma_2+1)\eta}{2(1-\eta)^3}\right] \\ &+ \frac{\alpha}{b^2}\left(T\frac{d\alpha}{dT}\right)^2\left[\frac{(6\gamma_2 - \gamma_1 - 1)\eta^4 + 2(2 - \gamma_1 - 4\gamma_2)\eta^3 + 7\gamma_2\eta^2 - 2\gamma_2\eta}{(1-\eta)^4}\right. \\ &\left. - 2\gamma_2 \ln(1-\eta)\right] + \frac{\alpha}{b}T^2\frac{d^2b}{dT^2} \\ &\times\left[(\gamma_2 \ln(1-\eta) + \frac{(5\gamma_2 - \gamma_1 - 1)\eta^3 + (3 - \gamma_1 - 5\gamma_2)\eta^2 + 2\gamma_2\eta}{2(1-\eta)^3}\right]\Bigg\} \\ &+ \frac{5}{2} + \left(\frac{h\nu}{kT}\right)^2 \frac{e^{h\nu/kT}}{(e^{h\nu/kT} - 1)^2} \end{aligned} \tag{18}$$

The heat capacity at constant pressure can be obtained through the thermodynamic relation,

$$C_p = C_v + \frac{T\alpha_T^2}{\beta\rho} \tag{19}$$

where α_T is the thermal expansion and β is the isothermal compressibility. The parameters α_T and β are defined as

$$\alpha_T = \frac{-1}{\rho}\left(\frac{\partial\rho}{\partial T}\right)_p \qquad \text{and} \qquad \beta = \frac{1}{\rho}\left(\frac{\partial\rho}{\partial p}\right)_T \tag{20}$$

The following formulas have been obtained from the equation of state for the parameters α_T and β.

$$\alpha_T = \left\{ \frac{dB_2}{dT} + \frac{d\alpha}{dT}\left[G(\eta) - 1 \right] + \frac{p}{\rho^2 k T^2} + \frac{\alpha}{\beta}\frac{db}{dT}\left[\frac{3\eta G(\eta)}{1-\eta} + \frac{2\gamma_2\eta^2 - \gamma_1\eta}{(1-\eta)^3} \right] \right\} \Big/ \times \left\{ 2\rho + \rho k T \left[-1 + \alpha\rho \left[\frac{3\eta G(\eta)}{1-\eta} + \frac{2\gamma_2\eta^2 - \gamma_1\eta}{(1-\eta)^3} \right] \right] \right\} \tag{21}$$

and

$$\beta = \left\{ 2\rho + \rho k T \left[-1 + \alpha\rho \left[\frac{3\eta G(\eta)}{1-\eta} + \frac{2\gamma_2\eta^2 - \gamma_1\eta}{(1-\eta)^3} \right] \right] \right\}^{-1} \tag{22}$$

The heat capacities can be calculated from Eqs. (1), (18), (19), (21), and (22). The calculated isobars of heat capacity at constant pressure and the ratio of heat capacities over the temperature range of 100 to 500 K are shown in Figs. 6 and 7, respectively, and are compared with the calculated values in Ref. 10. The maximum deviations which are due to the liquid–vapor phase transition extend to $\pm 31\%$.

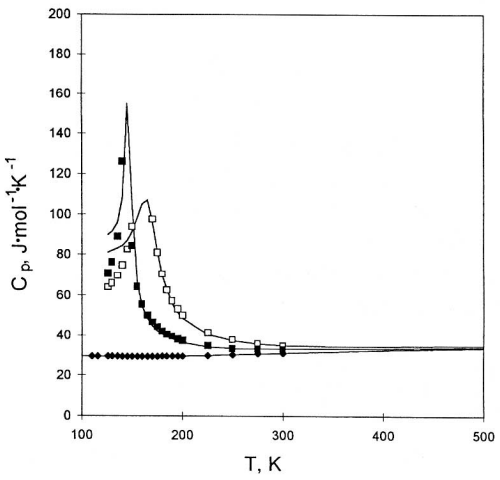

Fig. 6. The isobaric heat capacity, C_p, as a function of temperature at 1 bar (◆), 50 bar (■), and 100 bar (□). The curves represent the equation of state, and the points are taken from Ref. 10.

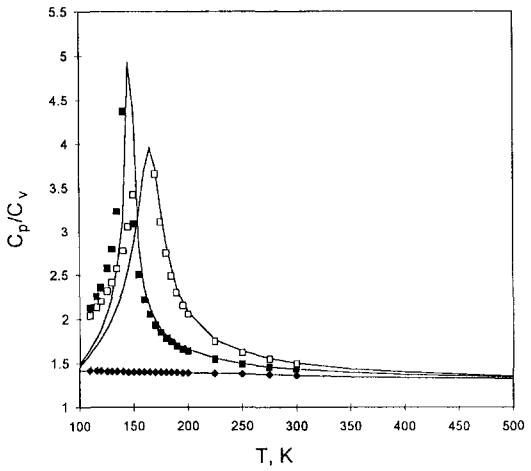

Fig. 7. Same as Fig. 6 for the ratio of heat capacities, C_p/C_v.

3.1.6. Joule–Thomson Coefficient and Joule–Thomson Inversion Curve

The Joule–Thomson coefficient has been proposed as a very sensitive test of the equation of state [13]. The Joule–Thomson coefficient, μ_{JT}, is related to the equation of state by the thermodynamic formula,

$$\mu_{JT} = \frac{T\alpha_T - 1}{\rho C_p} \tag{23}$$

Isobars of the Joule–Thomson coefficient have been calculated with Eqs. (1), (18), (19), (21), (22), and (23) and they are compared with the calculated values of Ref. 10 in Fig. 8. The average absolute error for the lower-pressure isobar is 6.6%.

The inversion curve is determined by the condition, $\mu_{JT} = 0$. For the present equation of state this yields

$$T\frac{dB_2}{dT} - B_2 + \left(\frac{T\,d\alpha}{dT} - \alpha\right)[G(\eta) - 1] + \alpha\left(\frac{1}{b}T\frac{db}{dT} - 1\right)\left[\frac{3\eta G(\eta)}{1-\eta} + \frac{2\gamma_2\eta^2 - \gamma_1\eta}{(1-\eta)^3}\right] = 0 \tag{24}$$

The calculated Joule–Thomson inversion curve is shown in Fig. 9 and is compared with a few available tabulated data [10].

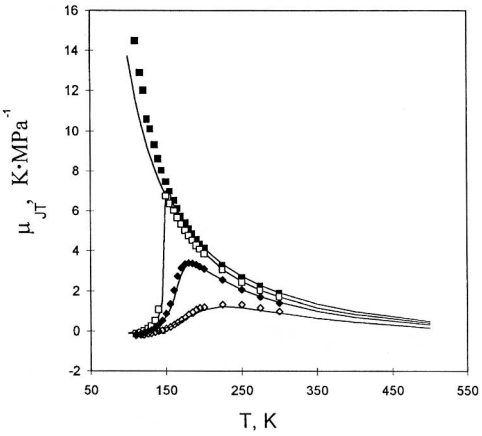

Fig. 8. Same as Fig. 6 for the Joule–Thomson coefficient, μ_{JT}, at 1 bar (■), 50 bar (□), 100 bar (◆), and 200 bar (◇).

3.1.7. Speed of Sound

The speed of sound can be calculated from the equation

$$W = \left[\frac{C_p}{C_v} \frac{1}{M} \left(\frac{\partial p}{\partial \rho} \right)_T \right]^{1/2} \tag{25}$$

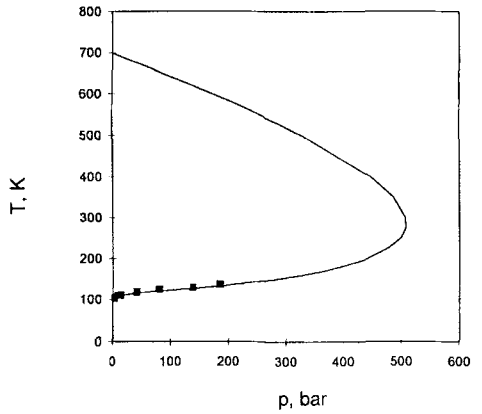

Fig. 9. The Joule–thomson inversion curve for fluorine. The curve represents the present equation of state, and the dots are taken from Ref. 10.

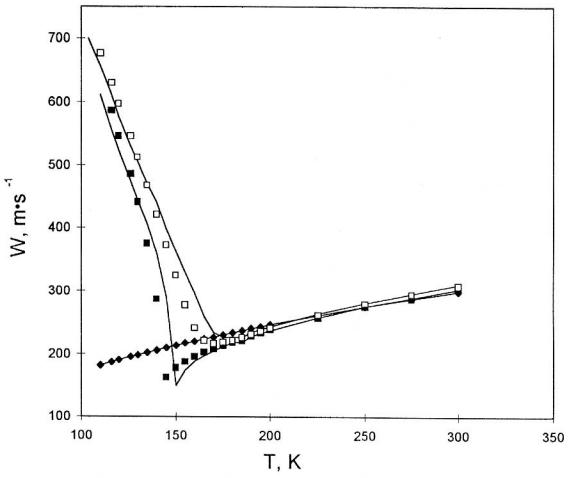

Fig. 10. Same as Fig. 6 for the speed of sound.

where W is the speed of sound and M is the molar mass. Equations (25) and (1) together with the experimental values of C_p/C_v have been used to calculate the speed of sound in fluorine. The calculated isobars of the speed of sound are shown in Fig. 10 and compared with the calculated data in Ref. 10. For the higher-pressure isobars, the maximum deviations extend to $\pm 26\%$.

3.2. Thermodynamic Properties in the Saturation State

3.2.1. Critical Constants

The critical constants can be found by the conditions $(\partial p/\partial v)_T = 0$ and $(\partial^2 p/\partial v^2)_T = 0$. These result in the following equations:

$$kT\alpha\rho\left[2\gamma_2\eta^2 - \gamma_1\eta + 3\frac{\eta}{1-\eta}(1-\gamma_1+\gamma_2\eta^2)\right] + (2p/\rho - kT)(1-\eta)^3 = 0 \tag{26}$$

and

$$kT\alpha\left[6\gamma_2\eta^2 - 2\gamma_1\eta + 3\frac{\eta}{1-\eta}(2-4\gamma_1\eta+6\gamma_2\eta^2) + 12\left(\frac{\eta}{1-\eta}\right)^2(1-\gamma_1\eta+\gamma_2\eta^2)\right] - 2p/\rho^2(1-\eta)^3 = 0 \tag{27}$$

Equations (26) and (27) solved simultaneously with Eq. (1) give the critical constants. We have found $T_c = 150$ K, $\rho_c = 12.53$ mol · L^{-1}, and $p_c = 50$ bar. The actual values of T_c, ρ_c, and p_c are 144.414 K, 15.60 mol · L^{-1}, and 52.395 bar, respectively [10]. Since the present equation of state is based on a mean-field approximation, the obtained critical constants cannnot be very accurate.

3.2.2. Vapor–Pressure Curve

The Maxwell construction on the p–v isotherms leads to the following equation:

$$\frac{p_{sat}}{kT}\left(\frac{1}{\rho_g}-\frac{1}{\rho_l}\right)=\ln\frac{\rho_l}{\rho_g}+(B_2-\alpha)(\rho_l-\rho_g)+\frac{\alpha}{b}(1+3\gamma)$$
$$\times\left[\gamma_2\ln\left(\frac{1-\eta_g}{1-\eta_l}\right)+(\gamma_1-2\gamma_2)\left(\frac{1}{1-\eta_l}-\frac{1}{1-\eta_g}\right)\right.$$
$$\left.+\frac{\gamma_2-\gamma_1+1}{2}\left(\frac{1}{(1-\eta_l)^2}-\frac{1}{(1-\eta_g)^2}\right)\right] \tag{28}$$

Solved simultaneously with the equation of state, this yields the saturated vapor pressure, p_{sat}, and the orthobaric liquid and vapor densities, ρ_l and ρ_g. The calculated vapor–pressure curve for fluorine is compared with the calculations of de Reuck [10] in Fig. 11, as $\ln p$ vs $1/T$ (in dimensionless

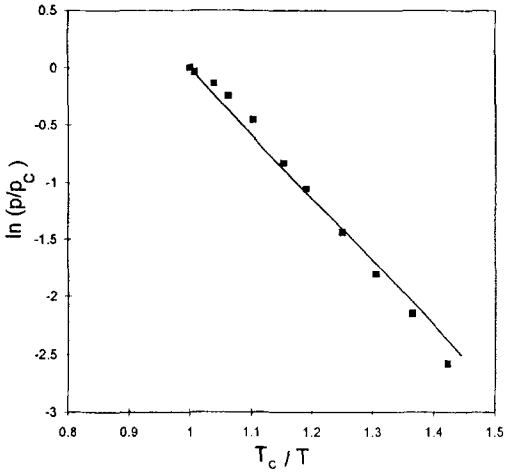

Fig. 11. Clausius–Clapeyron plot of $\ln p$ versus $1/T$ in dimensionless units. The curve is from Ref. 10, and the points represent our equation of state.

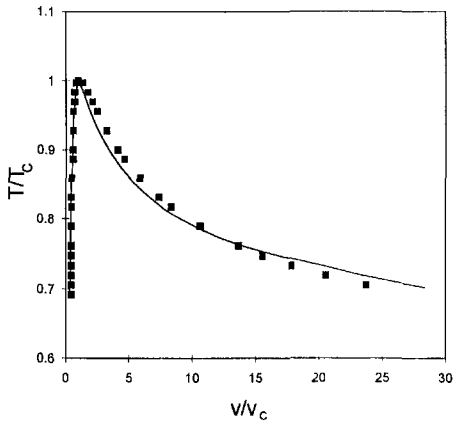

Fig. 12. The reduced orthobaric liquid and vapor volumes from 100 K to the critical point. The curve represents the equation of state, and the points are taken from Ref. 10.

units) over the temperature range of 100 K to the critical point. The average absolute deviation is 5.9%. The calculated orthobaric volumes from Eqs. (1) and (28) are compared with the calculated values of Ref. 10 in Fig. 12. Also shown in Fig. 13 are the calculated values of compressibility factor for the coexisting liquid and vapor phases and their

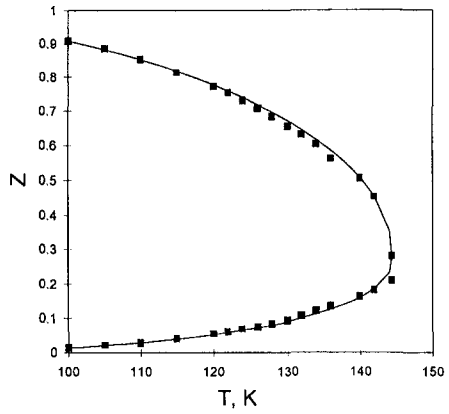

Fig. 13. The compressibility factors of the coexisting liquid and vapor phases as a function of temperature. The curve represents the equation of state, and the points are taken from Ref. 10.

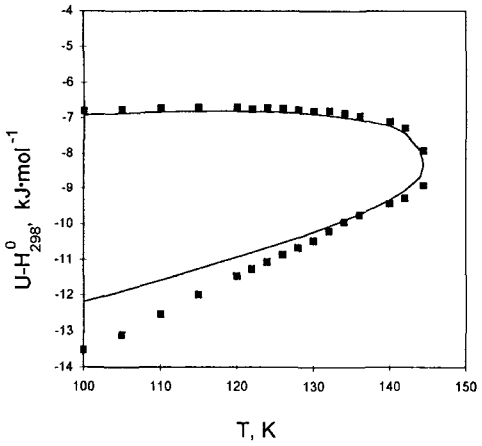

Fig. 14. The internal energy of the coexisting liquid and vapor phases as a function of temperature. The points are the present equation of state, and the curve is taken from Ref. 10.

comparison with the calculated values in Ref. 10. The average absolute deviation is 2.95%.

3.2.3. Internal Energy and Enthalpy

The formula and the method of calculation of internal energy and enthalpy are given in Section 3.1.3. We have calculated the values of internal energy and enthalpy from Eqs. (12) and (13) relative to the molar enthalpy of the ideal gas at 298 K. The calculated molar internal energies and enthalpies from 100 K to the critical point are compared with the calculated values of de Reuck [10] in Figs. 14 and 15, respectively. The

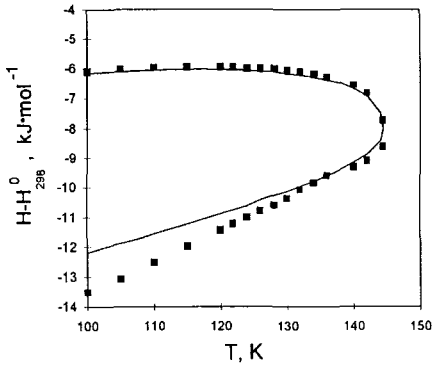

Fig. 15. Same as Fig. 14 for the enthalpy.

average absolute deviations are 2.80 and 2.93%, respectively. The Maxwell equal area construction has not been applied.

4. CONCLUSIONS

Our procedure provides a statistical–mechanical equation of state for fluorine in the compressed and liquid–vapor coexistence regions. Some of the previously proposed equations of state in the literature for fluorine consist of many terms that complicate the form of the equation and consequently all the related thermodynamic parameters. Usually these equations need much input data and are not based on a molecular level theory, and their complicated form does not allow direct physical interpretation. The present equation of state is accurate and simple in form, needs less input data, and has a statistical–mechanical basis. The temperature-dependent parameters of the equation of state can be calculated from three sets of integrations if the intermolecular pair potential is known. If the pair potential is not known, experimental knowledge of the second virial coefficient suffices to fix the Boyle parameters, from which $\alpha(T)$ and $b(T)$ can be calculated with sufficient accuracy from some simple model of the mean pair potential. Then γ is found empirically from limited information on the high-density fluid. Thus, a knowledge of the second virial coefficient plus some high-density data is sufficient to put the equation in the operative mode.

Our calculated results on the compressibility factor, fugacity coefficient, enthalpy, entropy, and Joule–Thomson coefficient are in very good agreement with the calculated values in Ref. 10. Higher deviations at low temperatures can be attributed to the inherent inaccuracies in the experimental low-temperature second virial coefficients. The latter three quantities contain the first derivative of the temperature-dependent parameters of the equation of state, and hence, the errors become exaggerated. The heat capacity involves a second differentiation of the parameters, and consequently, the errors become several orders of magnitude exaggerated.

Some of the deviations in the calculated results can be attributed to the location of the point at which the liquid–vapor phase transition occurs. Because the present equation of state is based on mean-field theory, it does not work very well in the two-phase region and does not reproduce exactly the phase-transition pressures or temperatures. Since the thermodynamic parameters vary severely as the phase transition occurs, this can lead to substantial error.

The calculated results are less accurate in the critical region. The relative deviations in the critical temperature, pressure, and volume are 4, -6, and, -10%, respectively, compared to the experimental values in

Ref. 9. This in not bad for such a point as the critical point, for example, the experimentally measured critical density of Ref. 9 is 11% less than that of Ref. 10. The calculated orthobaric liquid and vapor densities, the Clausius–Clapeyron plot of $\ln p$ vs $1/T$, and the compressibility factors as shown in Figs. 11–13 are good. The calculated values of internal energy and enthalpies in the vicinity of the triple point are well reproduced for the gas phase but are less accurate for the liquid phase. Perhaps this deficiency could be attributed to the effective van der Waals covolume b (equivalent to an effective hard-sphere diameter d).

REFERENCES

1. H. Moissan, *Ann. Chim. Phys.* **19**:272 (1891).
2. C. Gray and K. E. Gubbins, *Theory of Molecular Fluids, Vol. 1. Fundamentals* (Oxford University Press, Oxford, 1984).
3. B. M. Landanyi and D. Chandler, *J. Chem. Phys.* **62**:4308 (1975).
4. T. Boublik, *Mol. Phys.* **32**:1737 (1990).
5. Y. Song and E. A. Mason, *J. Chem. Phys.* **91**:7840 (1989).
6. Y. Song and E. A. Mason, *Phys. Rev. A* **42**:4743, 4749 (1990).
7. Y. Song and E. A. Mason, *Phys. Rev. A* **41**:3121 (1990).
8. J. H. Dymond and E. B. Smith, *The Virial Coefficient of Pure Gases and Mixtures. A Critical Compilation* (Oxford University, Oxford, 1980).
9. N. B. Vargaftik, *Handbook of Physical Properties of Liquids and Gases*, 2nd ed. (Hemisphere, Washington, DC, 1983).
10. K. M. de Reuck (ed), *IUPAC Fluorine International Thermodynamic Tables of the Fluid State-11* (Blackwell Scientific, Oxford 1990), p. 60.
11. D. A. McQuarre, *Statistical Mechanics* (Harper Collins New York, 1976).
12. S. N. Suchard and J. E. Metzer (eds.), *Spectroscopic Data, Vol. 2.* (Plenum London, 1976).
13. D. G. Miller, *Ind. Eng. Chem. Fundam.* **9**:585 (1970).